International Journal of Electrical and Electronics Engineers
Vol. No. 8, Issue No. 02, July-December 2016
ISSN (O) 2321-2055
ISSN (P) 2321-2045

A NOVEL HIGH STEP-UP CONVERTER BASED ON THREE WINDING COUPLED INDUCTOR FOR FUEL CELL ENERGY SOURCE APPLICATIONS

Thurai Chaitanya[1], V.Satyanarayana[2]

[1]*EEE Branch, Vaagdevi College of Engineering, Bollikunta, (India)*

[2]*EEE Department, Vaagdevi College of Engineering, Bollikunta, (India)*

ABSTRACT

This paper presents a high step-up converter for fuel cell energy source applications. The proposed high step-up dc–dc converter is devised for enhancing the voltage generated from fuel cell to be a 400-V dc-bus voltage. Through the three-winding coupled inductor and voltage doubler circuit, the proposed converter achieve high step-up voltage gain while not large duty cycle. The passive lossless clamped technology not only recycles leakage energy to improve efficiency but also alleviates large voltage spike to limit the voltage stress. Finally, the electric cell as input voltage supply 60–90 V integrated into a 2-kW epitome convertor was enforced for performance verification.

Index Terms—*Coupled inductor, fuel cell energy source applications, high step-up converter.*

I. INTRODUCTION

Recently, the cost increase of fossil fuel and new regulations of co_2 emissions have strongly increased the interests in renewable energy sources. Hence, renewable energy sources like fuel cells, solar energy, and wind power are widely valued and used. Fuel cells are considered as an excellent candidate to replace the conventional diesel/gasoline in vehicles and emergency power sources. Fuel cells will give clean energy to users while not co2 emissions. Because of stable operation with high-efficiency and sustain-able/renewable fuel supply, fuel cell has been increasingly accepted as a competently alternative source for the future [1], [2]. the excellent features like small size and high conversion efficiency make them valuable and potential. Hence, the fuel cell is suitable as power supplies for energy source applications [3]-[10].

International Journal of Electrical and Electronics Engineers
Vol. No. 8, Issue No. 02, July-December 2016
ISSN (O) 2321-2055
ISSN (P) 2321-2045

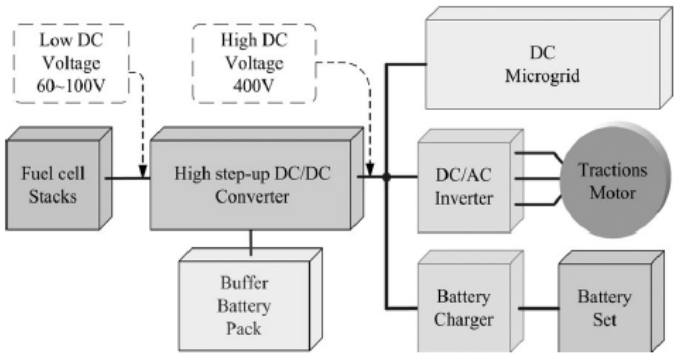

Fig. 1.Fuel cell power supply system with high step-up converter.

Generally speaking, a typical fuel cell power supply system containing a high step-up converter is shown in Fig. 1. The generated voltage of the fuel cell stack is rather low. Hence, a high step-up converter is strongly needed to lift the voltage for applications like dc microgrid, inverter, or battery.

Ideally, a conventional boost converter is able to achieve high step-up voltage gain with an extreme duty cycle. In practice, the step-up voltage gain is limited by effects of the power switch, rectifier diode, and also the resistances of the inductors and capacitors. in addition, the extreme duty cycle can result in a serious reverse-recovery problem and conduction losses. A flyback converter is able to achieve high step-up voltage gain by adjusting the turn's ratio of the transformer winding. However, a large voltage spike leakage energy causes can destroy the main switch. so as to protect the switch devices and constrain the voltage spike, a high-voltage-rated switch with high on-state resistance ($R_{D\ S\ -O\ N}$) and a snubber circuit are typically adopted in the flyback converter, however the leakage energy still be consumed.

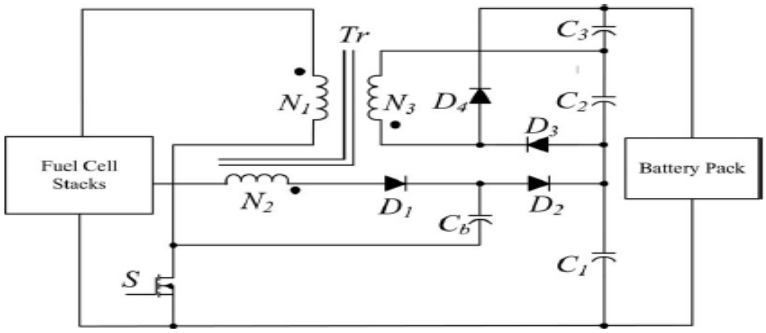

Fig. 2. Proposed high step-up converter.

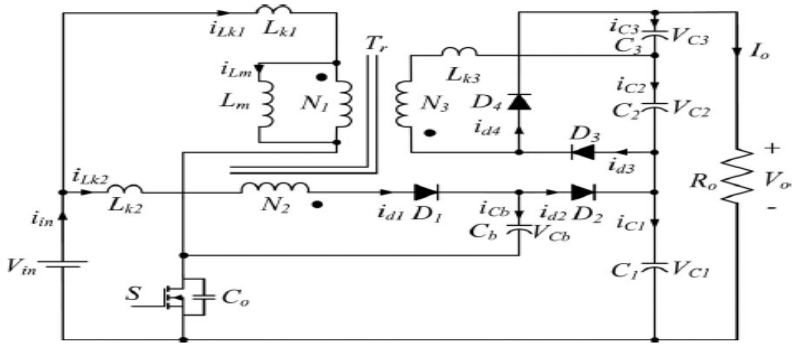

Fig. 3.Equivalent circuit of the proposed converter.

International Journal of Electrical and Electronics Engineers
Vol. No. 8, Issue No. 02, July-December 2016
ISSN (O) 2321-2055
ISSN (P) 2321-2045

These strategies can diminish the power conversion efficiency. so as to increase the con-version efficiency and voltage gain, several technologies like zero-voltage switching (ZVS), zero-current switching (ZCS), coupled inductor, active clamp, etc. are investigated. Some high step-up voltage gain will be achieved by using switched-capacitor and voltage-lift techniques, although switches can suffer high current and conduction losses. In recent years, coupled-inductor technology with performance of leakage energy recycle is developed for adjustable voltage gain; therefore, several high step-up converters with the characteristics of high voltage gain, high efficiency, and low voltage stress are given.. In this project, the presented high step-up converter designed for fuel cell energy source applications is shown in Fig. 2.

II. OPERATING PRINCIPLE OF THE PROPOSED CONVERTER

The proposed converter employs a switched capacitor and a voltage-doubler circuit for high step-up conversion ratio. The switched capacitor supplies an extra step-up performance; the voltage-doubler circuit lifts of the output voltage by increasing the turn's ratio of coupled-inductor.

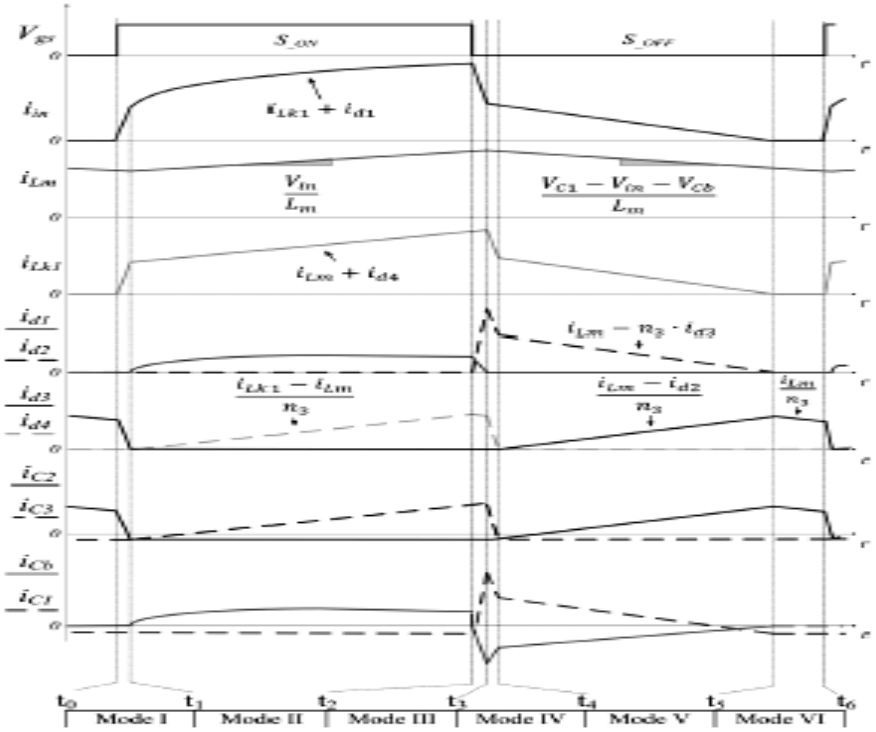

Fig. 4. Steady-state waveforms in CCM operation.

The advantages of proposed converter are as follows:

1) through adjusting the turns ratio of coupled inductor, the proposed converter achieves high step-up gain that renew-able energy systems require;
2) leakage energy is recycled to the output terminal, which improves the efficiency and alleviates large voltage spikes across the main switch;
3) due to the passive lossless clamped performance, the volt-age stress across main switch is substantially lower than the output voltage;

International Journal of Electrical and Electronics Engineers
Vol. No. 8, Issue No. 02, July-December 2016
ISSN (O) 2321-2055
ISSN (P) 2321-2045

4) low cost and high efficiency are achieved by adopting low-voltage-rated power switch with low R_{DS-ON};
5) by using three-winding coupled inductor, the proposed converter possesses more flexible adjustment of voltage conversion ratio and voltage stress on each diode.

The equivalent circuit of the proposed converter shown in Fig. 3 is composed of a coupled inductor T_r, a main power switch S, diodes D_1, D_2, D_3, and D_4, the switched capacitor C_b, and the output filter capacitors C_1, C_2, and C_3. L_m is the magnetizing inductor and L_{k1}, L_{k2}, and L_{k3} represent the leak-age inductors. The turns ratio of coupled inductor n_2 is equal to N_2/N_1, and n_3 is equal to N_3/N_1, where N_1, N_2, and N_3 are the winding turns of coupled inductor.

The steady-state waveforms of the proposed converter operating in CCM are depicted in Fig. 4. The each operating modes is shown in Fig. 5.

Mode I [t_0, t_1]: During this interval, the switch S is turned ON at t_0. The diodes D_1, D_2, and D_4 are reverse biased. The path of current flow is shown in Fig. 5(a). The primary leakage inductor current i_{Lk1} increases linearly, and the energy stored in magnetizing inductance still transfers to the load and output capacitor C_2 via diode D_3.

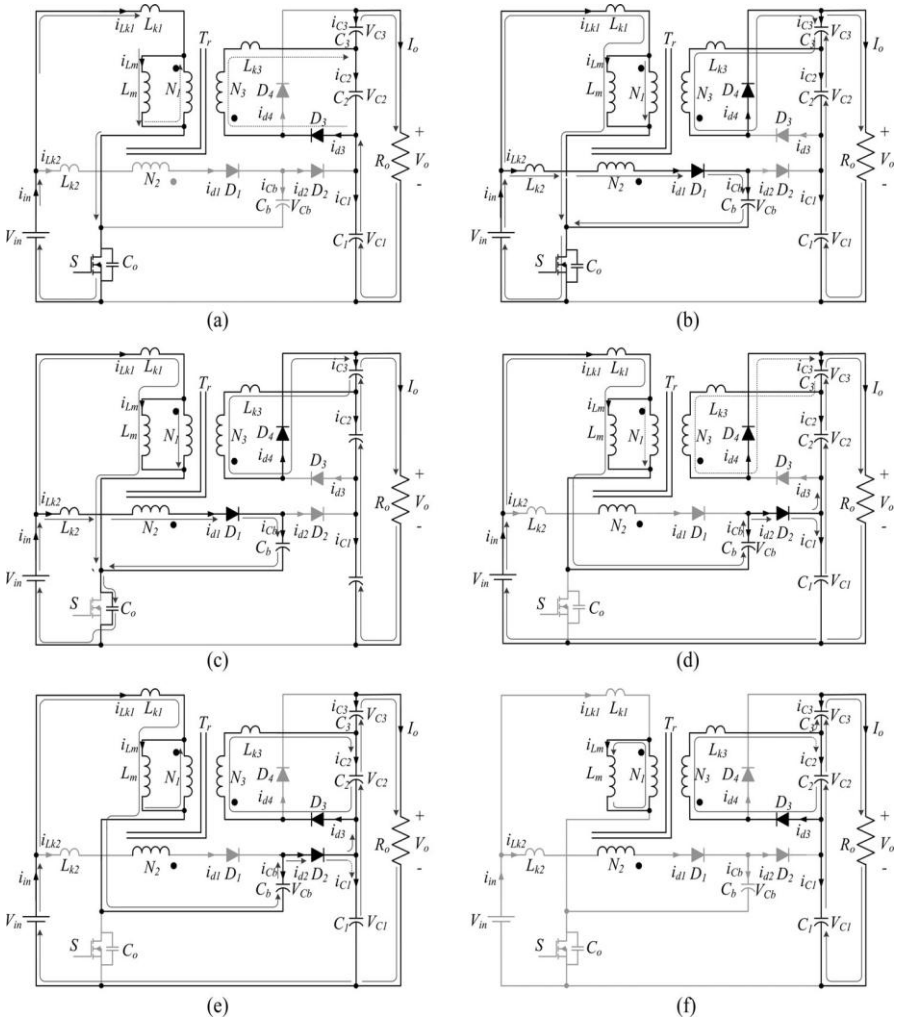

Fig. 5. CCM operating modes of the proposed converter. (a) Mode I [t_0 , t_1]. (b)Mode II [t_1 , t_2]. (c)Mode III [t_2 , t_3]. (d)Mode IV [t_3 , t_4]. (e)Mode V [t_4 , t_5]. (f) Mode VI [t_5 , t_6].

International Journal of Electrical and Electronics Engineers
Vol. No. 8, Issue No. 02, July-December 2016
ISSN (O) 2321-2055
ISSN (P) 2321-2045

Mode II [t_1, t_2]: During this interval, the switch S is still in the turn-on state. The diodes D_1 and D_4 are forward biased; diodes D_2 and D_3 are reverse biased. The path of current flow is shown in Fig. 5(b). The dc source V_{in} still charges into the magnetizing inductor L_m and leakage inductor $L_{k\,1}$, and the currents through these inductors rise linearly. Some of the energy from dc source V_{in} transfer to the secondary side of the coupled inductor to charge the capacitor C_3. The switched capacitor C_b is charged by the LC series circuit.

Mode III [t_2 , t_3]: During this interval, the switch S is turned OFF at t_2 . Diodes D_1 and D_4 are still forward biased; diodes D_2 and D_3 are reverse biased. The path of current flow is shown in Fig. 5(c). The magnetizing current and LC series current charge the parasitic capacitor C_o of the MOSFET.

Mode IV [t_3 , t_4]: During this interval, S is still in the turn-off state. The diodes D_1 , D_2 , and D_4 are forward biased. The diode D_3 is reverse biased. The current-flow path is shown in Fig. 5(d). The current i_{d4} charges the output capacitor C_3 and decreases linearly. The total voltage of V_{in} +V_{Lm} +V_{Cb} is charging to clamped capacitor C_1 , and some of the energy is supplied to the load.

Mode V [t_4 , t_5]: During this interval, switch S is still in the turn-off state. The diodes D_1 and D_4 are turned OFF; the diodes D_2 and D_3 are forward biased. The current-flow path is shown in Fig. 5(e). The energy of the primary side still charges to the clamped capacitor C_1 and supplies energy to the load. Some of the energy from dc source V_{in} is transferred to the secondary side of the coupled inductor to charge the capacitor C_2 , and the current i_{d3} increases linearly.

Mode VI [t_5 , t_6]: During this interval, switch S is still in the turn-off state. The diodes D_1, D_2, and D_4 are reverse biased; the diode D_3 is forward biased. The current-flow path is shown in Fig. 5(f). The current i_{Lk1} is dropped till zero. The magnetizing inductor L_m continuously transfers energy to the third leakage inductor $L_{k\,3}$ and the capacitor C_2 . The energies are discharged from C_1 and C_3 to the load. The current i_{d3} charges C_2 and supplies the load current.

III. STEADY-STATE ANALYSIS

In order to simplify the CCM steady-state analysis, the following factors are taken into account. All the leakage inductors of the coupled inductor are neglected, and all of components are ideal without any parasitic components. The voltages V_b , V_{C1} , V_{C2} , and V_{C3} are considered to be constant due to infinitely large capacitances.

3.1. Step-Up Gain

During the turn-on period of switch S, the following equations can be written as:

$$V_{C3} = V_{N3} = n_3 \cdot V_{\text{in}} \tag{1}$$

$$V_{Cb} = V_{\text{in}} + V_{N2} = (n_2 + 1) \cdot V_{\text{in}} \tag{2}$$

During the turn-off period of switch S, the following equations can be expressed as:

$$V_{C2} = n_3 \left[V_{C1} - (2 + n_2) \cdot V_{\text{in}} \right] \tag{3}$$

International Journal of Electrical and Electronics Engineers
Vol. No. 8, Issue No. 02, July-December 2016
ISSN (O) 2321-2055
ISSN (P) 2321-2045

$$V_{C1} = \left(\frac{D}{1-D} + 2 + n_2\right) \cdot V_{\text{in}} \tag{4}$$

Thus, the output voltage V_O can be expressed as

$$V_O = V_{C1} + V_{C2} + V_{C3} \tag{5}$$

By substituting (1), (3), and (4) into (5), the voltage gain of the proposed converter is given by

$$M_{\text{CCM}} = \frac{V_o}{V_{\text{in}}} = n_2 + \frac{2 - D + n_3}{1 - D} \tag{6}$$

Equation (6) shows that high step-up gain can be easily obtained by increasing the turns ratio of the coupled inductor without large duty cycle.

3.2. Voltage Stress

The voltage stress on the main switch is given as follows:

$$M_S = \frac{V_{S1}}{V_{\text{out}}} = \frac{1}{2 - D + (1 - D)\, n_2 + n_3}. \tag{7}$$

When the switching S is turned OFF, the diodes D_1 and D_3 are reverse biased. Therefore, the voltage stresses of D_1 and D_3 are as follows:

$$M_{D1} = \frac{V_{D1}}{V_{\text{out}}} = \frac{1 + n_2}{2 - D + (1 - D)\, n_2 + n_3} \tag{8}$$

$$M_{D4} = \frac{V_{D3}}{V_{\text{out}}} = \frac{n_3}{2 - D + (1 - D)\, n_2 + n_3}. \tag{9}$$

When the switch S is in turn-on period and the diodes D_2 and D_3 are reverse biased. Therefore, the voltage stresses of diodes

D_2 and D_3 are as follows:

$$M_{D2} = \frac{V_{D2}}{V_{\text{out}}} = \frac{1}{2 - D + (1 - D)\, n_2 + n_3} \tag{10}$$

$$M_{D3} = \frac{V_{D4}}{V_{\text{out}}} = \frac{n_3}{2 - D + (1 - D)\, n_2 + n_3}. \tag{11}$$

Equations (7)–(11) can be illustrated to determine the maximum voltage stress on each power drives.

3.3. Analysis of Conduction Losses

Some conduction losses are caused by resistances of semiconductor components and coupled inductor. Thus, all the components in the analysis of conduction losses are not continuously assumed to be ideal, except for all the capacitors. Diode reverse recovery problems, core losses, switching losses, and the ESR of capacitors are not discussed in this section. The characteristics of leakage inductor are disregarded because of energy recycling. The corresponding equivalent circuit includes copper resistances r_{L1}, r_{L2}, and r_{L3}, all the diode forward resistances r_{D1}, r_{D2}, r_{D3} , and r_{D4} , and the on-state resistance $R_{\text{DS-ON}}$ of the power switch.

International Journal of Electrical and Electronics Engineers
Vol. No. 8, Issue No. 02, July-December 2016
ISSN (O) 2321-2055
ISSN (P) 2321-2045

TABLE 1

Comparison between Three-Winding Coupled Inductor High Step-Up Converters

Converter Type	$M = \frac{V_{out}}{V_{in}}$	$M_S = \frac{V_{DS}}{V_{out}}$
Proposed converter	$n_2 + \frac{2 - D + n_3}{1 - D}$	$\frac{1}{1 + (n_2 + n_3) \cdot D + n_2 \cdot (1 - D)}$
Converter in [37]	$n_3 + \frac{1 + (n_2 + n_3) \cdot D}{1 - D}$	$\frac{1}{1 + n_3 \cdot D + (1 + n_3) \cdot (1 + D)}$
Converter in [39]	$(1 + n_2) + \frac{1 + D \cdot n_3}{1 - D}$	$\frac{1}{2 - D + n_2 \cdot (1 - D) + n_3}$

Table -2

Components Parameters of the Presented Converter

Part		Specifications
Input DC voltage		60-90 V
Output DC voltage		400 V
Maximum output power		5 A
Switching frequency		50 kHz
Current Mode PWM Controller		UC3845
Coupled inductors turns ratio		N_1:N_2:N_3=1:1:1.5
Magnetizing inductor		170uH
Main power MOSFET		IXFN 130N30 300V, 130A, 22mΩ
Diodes	D_1	DSEP30-06A 600V, 30A
	$D_2/D_3/D_4$	MBR20200CT 200V, 20A
Capacitors	C_b	220uF/200V
	C_1	220uF/200V
	C_2/C_3	470uF/450V

3.4. Comparison Between the Proposed Converter and the Other High Step-Up Converters

The performance of the proposed converter is verified by an analytical comparison with other three-winding coupled inductor high step-up converters for fuel cell, and it is assumed that all the converters are operated in CCM. Moreover, for the sake of fair comparison, the analysis will also assume that the input voltage and the turns ratios of coupled inductor are the same: n_2 = 1.5; n_3 = 1.5. Table I summarizes the voltage conversion ratio and the switch stress for the proposed converter and the other single switch high step-up converter topologies introduced.

In this comparison between the proposed converter and other converter, n2 is defined as the turns ratio N_2 /N_1 ; and n3 is defined as the turns ratio N_3 /N_1 .

The comparison of voltage gain and the switch stress between the three-winding coupled inductor high step up converters. The voltage gain of the proposed converter is higher than that of the other high step-up converters at duty cycle of 0.1< D < 0.6. The voltage stress of switch of the proposed converter is lower than that of other high step-up converter at duty cycle of 0.1 < D < 0.6. This is a very attractive feature because the low-voltage-

International Journal of Electrical and Electronics Engineers
Vol. No. 8, Issue No. 02, July-December 2016
ISSN (O) 2321-2055
ISSN (P) 2321-2045

rated MOSFET with lower RDS-ON can be adopted to improve the efficiency. Under D >0.6, although the voltage gain of the proposed converter is not the highest and the voltage stress of the proposed converter is not the lowest, the operation under large duty cycle D >0.6 resulting in low efficiency will not be designed in reasonable consideration.

IV. SIMULATION RESULTS

The presented converter for fuel cell input source, prototype circuit is tested to verify the performance.

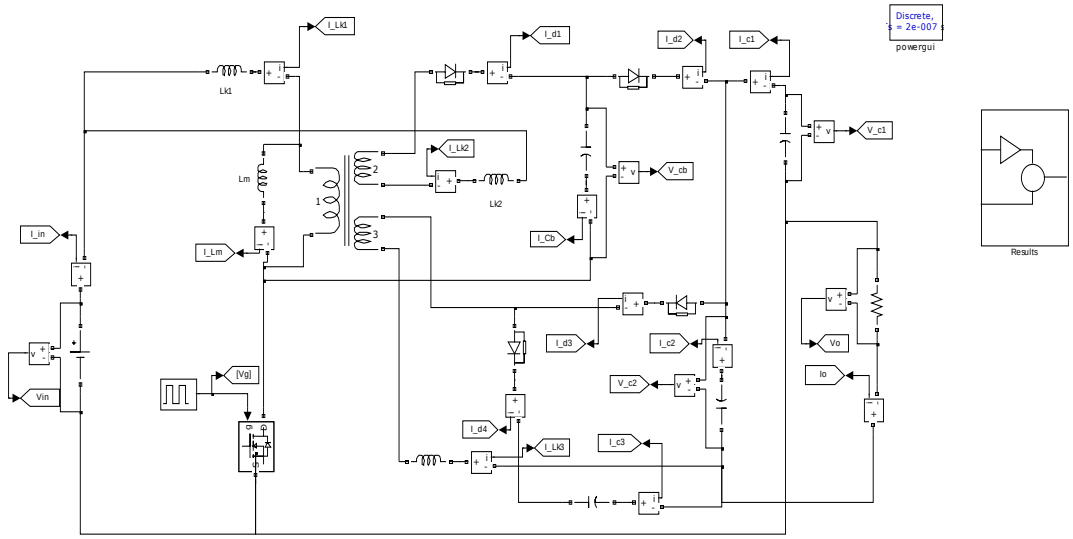

Fig.6.Simulation Model

The range of duty cycle D under input voltage 60–90 V is designed as 0.2–0.5 and the turn's ratio n_1:n_2:n_3 is selected as 1:1:1.5. The leakage inductance L_{k1} is measured as 3.3 μH. All of the major components parameters of the prototype used for simulation are presented in Table II. Simulation results are shown in figure 7, 8 and 9.

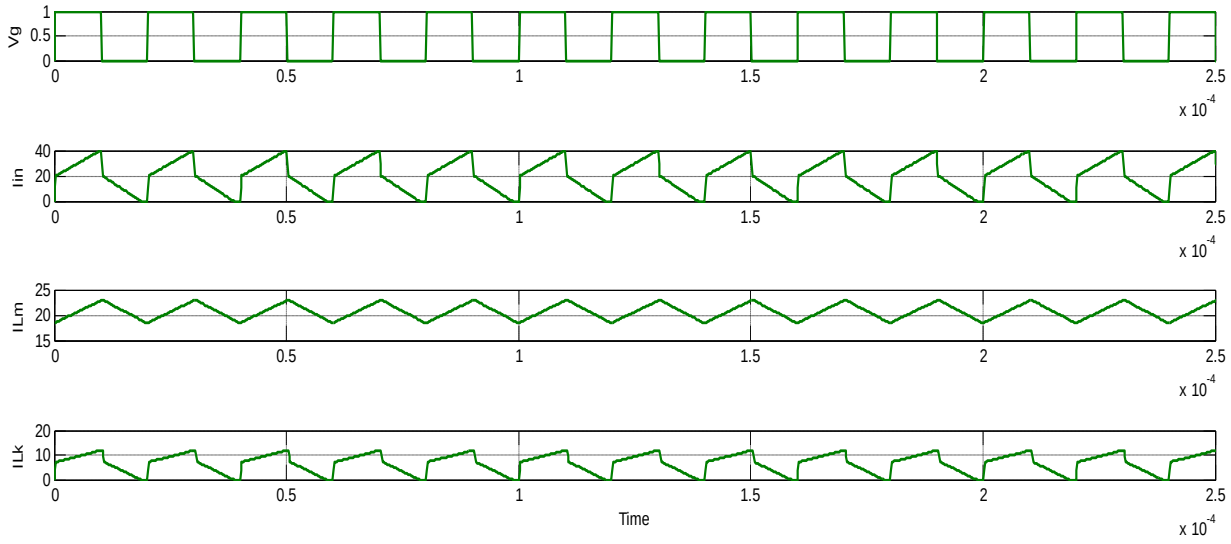

Fig.7. Simulation results for V_g, I_{in},I_{Lm} and I_{Lk}

International Journal of Electrical and Electronics Engineers
Vol. No. 8, Issue No. 02, July-December 2016
ISSN (O) 2321-2055
ISSN (P) 2321-2045

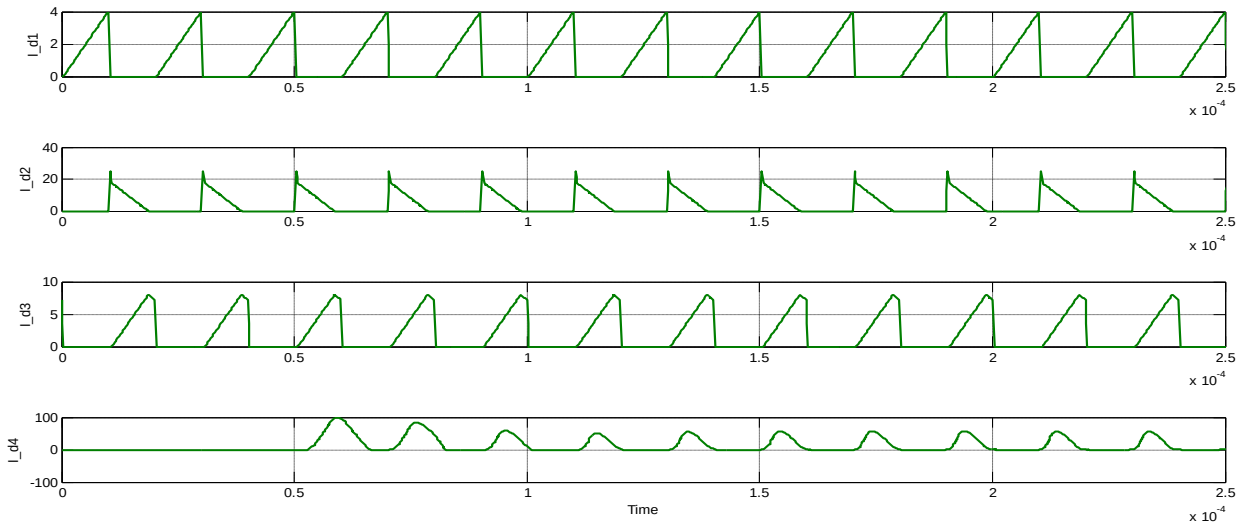

Fig.8. Simulation results for I_{d1}, I_{d2}, I_{d3} and I_{d4}

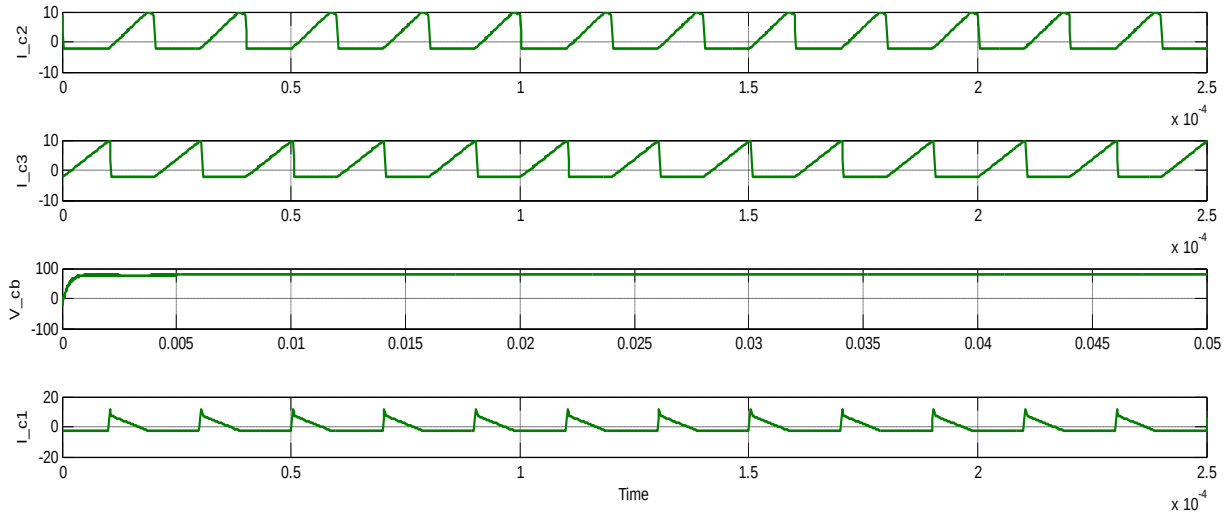

Fig.9. Simulation results for I_{c2}, I_{c3}, V_{cb} and I_{c1}

V. CONCLUSION

In this project, a high step-up dc–dc converter for fuel cell hydroid electric vehicle applications is clearly analyzed and successfully verified. By employing technologies of three-winding coupled inductor, switched capacitor, and voltage doubler circuit, the high step-up conversion will be efficiently obtained. The leakage energy is recycled and large voltage spike is alleviated; thus, the voltage stress is limited and also the efficiency is improved. The full-load efficiency is up to 91.32% and also the maximum efficiency is up to 96.81%. The voltage stress on the main switch is clamped as 120 V at D_{max} . The low-voltage-rated switch with low R_{DS-ON} will be chosen for the reduction of conduction losses. Thus, the proposed device is suitable for high-power applications as fuel cell systems in hydroid electric vehicles.

REFERENCES

[1] W. Li, X. Lv, Y. Deng, J. Liu, and X. He, "A review of non-isolated high step-up DC/DC converters in renewable energy applications," in Proc. IEEE Appl. Power Electron. Conf. Expo., Feb. 2009, pp. 364–369.

[2] W. Li and X. He, "Review of nonisolated high-step-up DC/DC converters in photovoltaic grid-connected applications," IEEE Trans. Ind. Electron., vol. 58, no. 4, pp. 1239–1250, Apr. 2011.

[3] M. A. Laughton, "Fuel cells," IEE Eng. Sci. Edu. J., vol. 11, no. 1, pp. 7– 16, Feb. 2002.

[4] W. Jiang and B. Fahimi, "Active current sharing and source management in fuel cell-battery hybrid power system," IEEE Trans. Ind. Electron., vol. 57, no. 2, pp. 752–761, Feb. 2010.

[5] P. Thounthong, S. Rael, and B. Davat, "Analysis of supercapacitor as second source based on fuel cell power generation," IEEE Trans. Ind. Electron., vol. 24, no. 1, pp. 247–255, Mar. 2009.

[6] A. Khaligh and Z. Li, "Battery, ultracapacitor, fuel cell, and hybrid energy storage systems for electric, hybrid electric, fuel cell, and plug-in energy source applications: State of the art," IEEE Trans. Veh. Technol., vol. 59, no. 6, pp. 2806–2814, Jul. 2010.

[7] L. Wang and H. Li, "Maximum fuel economy-oriented power management design for a fuel cell vehicle using battery and ultracapacitor," IEEE Trans. Ind. Appl., vol. 46, no. 3, pp. 1011–1020, May/Jun. 2010.

[8] M. Marchesoni and C. Vacca, "New DC–DC converter for energy storage system interfacing in fuel cell energy source applications," IEEE Trans. Power. Electron., vol. 22, no. 1, pp. 301–308, Jan. 2007.

[9] G.-J. Su and L. Tang, "A reduced-part, triple-voltage DC-DC converter for EV/HEV power management," IEEE Trans. Power Electron., vol. 24, no. 10, pp. 2406–2410, Oct. 2009.

[10] S. M. Dwari and L. Parsa, "A novel high efficiency high power interleaved coupled-inductor boost DC–DC converter for hybrid and fuel cell electric vehicle," in Proc. IEEE Veh. Power Propulsion Conf., Sep. 2007, pp. 399– 404.